Available online at www.sciencedirect.com
SCIENCE DIRECT®
Nuclear Physics A 741 (2004) 60–77
NUCLEAR PHYSICS A
www.elsevier.com/locate/npe

The coupling between the IAS and the IMS

D.R. Bes [a,b], O. Civitarese [c,*]

[a] *Departamento de Física, CNEA, av. Libertador 8250, (1429) Buenos Aires, Argentina*
[b] *Departamento de Física, Universidad Favaloro, Belgrano 1723, (1093) Buenos Aires, Argentina*
[c] *Departamento de Física, UNLP, C.C. 67, (1900) La Plata, Argentina*

Received 19 April 2004; received in revised form 10 June 2004; accepted 11 June 2004

Available online 8 July 2004

Abstract

In a previous paper we have studied the structure of the Isobaric Analogue State (IAS) using a realistic single-particle model within a formalism that allows to disentangle real effects of isospin violations from spurious effects associated with the construction of basis states. In this work we discuss the influence of the Isovector Monopole State (IMS) on the width of the IAS. According to our results, the presence of a collective IMS is necessary to preserve the empirically found isolation of the IAS from states of the background. This is valid for a simplified harmonic oscillator model and for a realistic single-particle basis as well, since for both cases there is a strong Coulomb mixing between the IAS and the IMS, which increases at the expense of decreasing the mixing between the IAS and the $\Delta N = 0$ configuration states. The prediction of the total width of the IAS remains in reasonable agreement with the experimental value in a calculation without free parameters.

PACS: 21.60.Jz; 22.40.Hc; 21.60.Fw

1. Introduction

In a previous paper (here on referred to as I) [1], we have been able to account for the width of the isobaric analogue state (IAS) in ^{208}Bi by means of a procedure that allows us to disentangle physical effects due to isospin non-conserving terms in the Hamiltonian from spurious effects arising from the presence of isospin impurities in the set of basis states. In that calculation the starting Hamiltonian consisted of pure single-

* Corresponding author.
E-mail address: civitare@fisica.unlp.edu.ar (O. Civitarese).

0375-9474/$ – see front matter
doi:10.1016/j.nuclphysa.2004.06.019

particle terms. In particular, a Woods–Saxon potential with spin–orbit coupling was used and no two-body terms were introduced (other than the counterterms demanded by the procedure).

However, at least in heavy nuclei, the width of the IAS ($T' = T$) has been attributed [2] to its mixture with the isovector monopole state (IMS) with $T' = T - 1$, due to the strong relation between the intrinsic structures of these two modes [3,4]. In turn, the IMS would decay to one-particle–one-hole and two-particle–two-hole states ($T' = T - 1$) lying in the vicinity of the IAS, thus yielding a width. Comparison with experimental data has been successfully performed using this approach [5]. However, quite a number of parameters have been introduced along this procedure, a fact which renders uncertain the validity of the model, no matter how useful it may be to provide a framework for the systematization of the experimental data.

Properties of the IMS have been studied by Auerbach and Klein using the self-consistent HF–RPA approach with Skyrme-type nucleon–nucleon interactions [6]. Calculations were made in **r**-coordinate representation, which is specially suitable for treating particles in the continuum. These authors have also derived sum rules for the three modes $\Delta T = 0, \pm 1$ and discussed blocking effects due to neutron excess.

Microscopic RPA calculations yield a width of the IAS, already at lowest order. In I, we have corrected the errors due to the fact that single-particle states used in the description of nuclei with a neutron excess do not carry the isospin as a good quantum number. The correction is performed through the introduction of collective coordinates in isospace. As shown in [7] this is the natural way to treat cases that violate a symmetry. Application of this procedure to the present case enables us:

(i) to restore the isospin symmetry of the problem;
(ii) to diagonalize within the RPA the subset of isospin $T - 1$ states, including the IMS, but excluding the IAS (with isospin T);
(iii) to isolate (to the same leading RPA order) the isospin non-conserving terms of the Hamiltonian; and
(iv) to perform an exact diagonalization of these last terms within the subset of RPA modes plus IAS.

In the present paper we pay special consideration to the role that the IMS plays in the width of the IAS. We use the same formalism as in I, but with the inclusion of a two-body interaction that is specific for the IMS.

2. The many-body framework

2.1. Single-particle states

Single-particle states are created by the operators $b^+_{\omega jm}$ for protons and $c^+_{\nu jm}$ for neutrons. Here ω, ν label states with the same orbital and total angular momenta; the label j includes the orbital angular momentum l.

We allow for the fact that the proton and neutron basis may be different. For instance, they may be obtained from Woods–Saxon potentials with different parameters for protons and neutrons.

The isospin operators should take into account the differences between the proton and neutron basis[1]

$$\tau_1 = -\frac{1}{\sqrt{2}} c^+_{p\nu jm} c_{\nu jm} = -\frac{1}{\sqrt{2}} x_{\nu\omega j} b^+_{\omega jm} c_{\nu jm},$$
$$\tau_{-1} = \frac{1}{\sqrt{2}} c^+_{\nu jm} c_{p\nu jm} = \frac{1}{\sqrt{2}} x_{\nu\omega j} c^+_{\nu jm} b_{\omega jm},$$
$$\tau_0 = \frac{1}{2}\left(x_{\omega\sigma j} x_{\sigma\nu j} b^+_{\omega jm} b_{\nu jm} - c^+_{\omega jm} c_{\nu jm}\right). \tag{1}$$

In the above expressions we denote by $c^+_{p\nu jm}$ the proton creation operator that is obtained from the neutron creation operator $c^+_{\nu jm}$ through the charge conjugation. It may be expanded in terms of the proton creation operators $b^+_{\omega jm}$ with the same values of j, m

$$c^+_{p\nu jm} = x_{\nu\omega j} b^+_{\omega jm}. \tag{2}$$

2.2. The Hamiltonian

We assume total and Coulomb single-particle Hamiltonians

$$H^{(e)}_{\rm sp} = e_{p\omega j} b^+_{\omega jm} b_{\omega jm} + e_{n\nu j} c^+_{\nu jm} c_{\nu jm}, \tag{3}$$
$$H^{(q)}_{\rm sp} = \langle p\omega j | V_{\rm coul} | p\sigma j\rangle b^+_{\omega jm} b_{\sigma jm}. \tag{4}$$

$H^{(e)}_{\rm sp}$ may display realistic single-particle energies. The ground state will be represented by a double-magic nucleus with neutron excess $2T$ and isospin projection $T_z = -T$.

In the present paper we also include an isospin scalar specific interaction for the IMS mode, namely

$$H_{\rm IMS} = -\frac{\alpha}{2}[S_1, S_1^-]_+, \tag{5}$$

where $S_{\pm 1}$ carries isospin 1 and isospin projection ± 1. Here

$$S_1 = -\frac{1}{\sqrt{2}} s_{\omega\nu j} b^+_{\omega jm} c_{\nu jm}, \tag{6}$$
$$s_{\omega\nu j} = -\sqrt{2}\langle p\omega jm | r^2 \tau_1 | n\nu jm\rangle. \tag{7}$$

The non-vanishing matrix elements $s_{\omega\nu j}$ are such that the labels ω, ν are always different ($\nu - \omega = \pm 1$).

If the Coulomb term is the only isospin symmetry breaking contribution, the difference

$$H^{(\epsilon)}_{\rm sp} = H^{(e)}_{\rm sp} - H^{(q)}_{\rm sp} \tag{8}$$

[1] We use the Einstein convention that the repetition of an index on a given side of an equation implies a summation over that index, unless the same index appears on the other side of the equation.

should be attributed to the Hartree–Fock contribution of an isospin conserving two-body interaction. Part of this interaction may be attributed to $H_{\rm IMS}$.

The one- and two-body terms of the Hamiltonian are treated within the RPA. The modes are labeled by the quantum number $t = \pm 1$, according to whether they increase or decrease the isospin projection T_z. In the case of $T_z = T - 1$ modes, the spectrum has three branches, associated with isospin $T + 1$, T and $T - 1$, respectively. Since the branch with isospin $T - 1$ carries most of the intensity [6], it is the only one considered in this work. Consistently, in the following we take into account the leading order term in the expansion of different contributions in powers of $1/T$ (see I).

In order to insure the essential overall isoscalar symmetry, we follow the treatment of the motion of the center of mass[2] developed in [8]. The detailed discussion of the formalism can be found in I. For the benefit of the reader we shall now briefly enumerate the main steps of the formalism, which are the following:

(i) the introduction of the counterterms which restore the isospin symmetry of the Hamiltonian (8);
(ii) the transformation of the resulting Hamiltonian to the intrinsic frame;
(iii) the application of Marshalek treatment of the collective space in terms of phonons; and
(iv) the determination of the elementary degrees of freedom and the coupling between them.

To begin with our treatment we add counterterms

$$H^{(\epsilon)} = H_{\rm sp}^{(\epsilon)} + H_{\rm IMS} - \mathcal{T}_1\tau_{\bar{1}} - \mathcal{T}_{\bar{1}}\tau_1. \tag{9}$$

The operators $\mathcal{T}_{\pm 1}$ are determined by the requirement that $H^{(\epsilon)}$ becomes invariant under isospin transformations. To leading order, this requirement leads to the expressions

$$\begin{aligned}
\mathcal{T}_{\pm 1} &= -\frac{1}{T}\big(H_{{\rm sp}1(\pm 1)}^{(\epsilon)} + \alpha\langle S_0\rangle S_{\pm 1} - \tau_{\pm 1}\langle\mathcal{T}_0\rangle\big),\\
\langle\mathcal{T}_0\rangle &= -\frac{1}{2T}\big(\langle H_{{\rm sp}10}^{(\epsilon)}\rangle + \alpha\langle S_0\rangle^2\big).
\end{aligned} \tag{10}$$

The total Hamiltonian is written

$$H = H_{\rm sp}^{(e)} + V, \tag{11}$$

$$V = H_{\rm IMS} - (\mathcal{T}_1\tau_{\bar{1}} + \mathcal{T}_{\bar{1}}\tau_1). \tag{12}$$

As in I, we must transform the Hamiltonian to the intrinsic frame. Therefore, it is relevant to determine the isomultipoles $(\lambda, \mu = 0)$ of each of its terms. Both single-particle Hamiltonians (3), (4) include isoscalar $H_{\rm sp00}$ and isovector $H_{\rm sp10}$ components. The two-body terms V in (9) display isoscalar and isoquadrupole terms

[2] The commonly used procedure of adjusting constants to ensure the appearance of a zero-energy root, may introduce significant errors in the population of the remaining modes through the operator τ_1, and thus in the calculation of the width of the IAS (see [8]).

$$V_{00} = -\frac{2}{3}(\mathcal{T}_1\tau_{\bar{1}} - \mathcal{T}_{\bar{1}}\tau_1) + \frac{2}{3}\mathcal{T}_0\tau_0 - \frac{\alpha}{3}[S_1, S_{\bar{1}}]_+ + \frac{\alpha}{3}S_0^2,$$
$$V_{20} = -\frac{1}{3}(\mathcal{T}_1\tau_{\bar{1}} - \mathcal{T}_{\bar{1}}\tau_1) - \frac{2}{3}\mathcal{T}_0\tau_0 - \frac{\alpha}{6}[S_1, S_{\bar{1}}]_+ - \frac{\alpha}{3}S_0^2. \tag{13}$$

3. Collective variables and constraints

The transformation parameters determining the orientation of an intrinsic frame of reference in isospace are raised to the status of collective coordinates. The total Hilbert space is thus factorized into intrinsic and collective subspaces.

$$\Psi = \psi_{\text{intrinsic}} \times \psi_{\text{collective}},$$
$$\psi_{\text{collective}} = \sqrt{\frac{2T+1}{8\pi^2}} D^T_{MK} \approx \frac{(\Upsilon^+)^{2T}(\xi^+)^m(\zeta^+)^k}{\sqrt{(2T)!m!k!}}|\rangle, \tag{14}$$

where T, M, K are the collective isospin and its projections along the laboratory and the intrinsic z-axis, respectively. In the Marshalek representation (14) $m = \frac{1}{2}(T+M)$, $k = \frac{1}{2}(T+K)$ [9]. This representation is specially useful for $m \ll T$ and $k \ll T$, which we assume to be the case. The operator ξ^+ increases the isospin projection in the laboratory frame by one unit, while ζ^+ performs the same task in the intrinsic frame. One also defines the isospin raising operator through the equation

$$\beta^2 \frac{(\Upsilon^+)^{2T}}{\sqrt{(2T)!}}|\rangle \equiv \frac{(\Upsilon^+)^{2T+2}}{\sqrt{(2T+2)!}}|\rangle. \tag{15}$$

The over-completeness of the Hilbert space requires the existence of compensating constraints

$$\tau_{0,\pm1} = T_{0,\pm1}. \tag{16}$$

To leading orders in an expansion in T^{-1}, these constraints are expressed by

$$\tau_0 = -T + \zeta^+\zeta, \qquad \tau_1 = -\sqrt{T}\zeta, \qquad \tau_{\bar{1}} = \sqrt{T}\zeta^+. \tag{17}$$

4. The elementary modes of excitation and the coupling terms

Every operator should be transformed to the intrinsic system, including the Hamiltonian. Using the expansion of the rotational matrix elements $D^\lambda_{\mu\nu}$ in terms of the operators β, ξ^+, ξ, ζ^+, ζ, one obtains the isospin conserving term H_t and the coupling term H_c (cf. [10])

$$H_t = W + \omega_\xi \xi^+\xi + \mathcal{O}\big(T^{-1/2}\big). \tag{18}$$

Repeated application of the operator ξ^+ generates the sequence of IAS. It is associated with the energy

$$\omega_\xi = -\frac{1}{T}\big\langle H^{(q)}_{\text{sp10}}\big\rangle \tag{19}$$

while the orthonormal modes with isospin $T-1$ are determined from the Hamiltonian

$$W = H_{\rm sp}^{(e)} + V + \frac{\omega_\xi}{2T}[\tau_1, \tau_{\bar{1}}]_+ + \frac{1}{T}\big(\Xi^+\tau_{\bar{1}} - \Xi\tau_1\big) + \mathcal{O}\big(T^{-1/2}\big),$$
$$\Xi^+ = H_{\rm sp11}^{(q)} + \frac{1}{T}\langle H_{\rm sp10}^{(q)}\rangle\tau_1 + \mathcal{O}\big(T^{-1/2}\big). \tag{20}$$

Both the Hamiltonian W (to be diagonalized within the RPA) and the operator Ξ^+ are expressed in terms of uncoupled creation and annihilation bosons. Since

$$[W, \tau_{\pm1}] = \big[\Xi^+, \tau_{\pm1}\big] = 0, \tag{21}$$

we expect to find a root with zero frequency corresponding to the isospin degree of freedom. Consistently, the operator Ξ^+ only displays matrix elements connecting the ground state with finite-frequency bosons. It means that the badly-behaved operator τ_1 is eliminated and replaced by the well-behaved collective operator ξ^+.

To the same RPA order, there appears a term

$$H_c = -\frac{1}{\sqrt{T}}\big(\beta^{-2}\xi\,\Xi^+ + \beta^2\xi^+\Xi\big) \tag{22}$$

which couples the finite RPA roots with the IAS. The operators $\beta^{\pm2}$ change the value of the isospin T according to (15). We diagonalize this interaction through the procedure advocated in Appendix 2D of Ref. [11].

The width of the IAS is determined by means of the population of the resultant states by means of the isospin operator τ_1. Since

$$\tau_1 \to \sqrt{T}\xi^+ + \mathcal{O}\big(T^{-1/2}\big), \tag{23}$$

this population is achieved through the admixtures of the IAS $\xi^+|\rangle$ in each final state.

5. Results

In the first place we apply the previous formalism to the case of a harmonic oscillator potential, neglecting $\mathbf{l}.\mathbf{s}$ and $\mathbf{l}^2$ contributions. Since in this model the $\Delta T_z = 1$ branch of excitations consists only of the IAS and the IMS, we profit from this schematic structure in order to study the coupling between these two modes. Next, we apply the formalism to a realistic situation, and we compare the resulting features with those of the schematic calculation and with experimental values.

5.1. Harmonic oscillator approximation

We consider nucleons moving in a pure harmonic oscillator potential with the same frequency ω for both neutrons and protons

$$H_{\rm sp}^{(e)} = \hbar\omega\big(b_{Njm}^+ b_{Njm} + c_{Njm}^+ c_{Njm}\big). \tag{24}$$

Since $[H_{\rm sp}^{(e)}, \tau_q] = 0$, then $x_{\nu\omega j} = \delta_{\nu\omega}$ in Eq. (2).

We denote by N_p the principal quantum number of the last shell filled with protons and by N_n the corresponding value for neutrons. We assume $N_n = N_p + 1$.

The particle–hole isovector monopole excitations are created by

$$\gamma^+_{1a'j} = \frac{1}{\sqrt{2}\hat{j}} b^+_{(N_{a'}+2)jm} c_{N_{a'}jm},$$
$$\gamma^+_{\bar{1}1j} = \frac{1}{\sqrt{2}\hat{j}} c^+_{(N_p+2)jm} b_{N_pjm}, \tag{25}$$

where $\hat{j} = \sqrt{j+1/2}$. There are three types of particle–hole isovector monopole operators carrying $\Delta N = 2$, $\Delta L = 0$, $\Delta T_z = 1$, which are labeled by $a' = 2, 3, 4$. In the first line of (25), $N_2 = N_n$; $N_3 = N_n - 2$, and $N_4 = N_p$ (see Table 3 of I). Similarly, there is only one type of excitations with $\Delta N = 2$, $\Delta L = 0$, $\Delta T_z = -1$, which is labeled by the index 1.

Within the spirit of the RPA, the Hamiltonian W is written in terms of the operators (25) (see Eq. (20)). The corresponding expression of the operator S_1 is

$$S_1^{(\mathrm{RPA})} = -\hat{j} A_{a'j} \gamma^+_{1a'j} - \hat{j} A_{pj} \gamma^-_{\bar{1}1j}, \tag{26}$$

where $A_{a'j} = A_{N_{a'}l}$ and $A_{pj} = A_{N_pl}$. Here

$$A_{Nl} \equiv \langle (N+2)lm_l | r^2 | Nlm_l \rangle = \frac{1}{2}\sqrt{(N-l+2)(N+l+3)}\frac{\hbar}{M\omega}. \tag{27}$$

We have also defined the sum rules Σ_N and their average Σ

$$\Sigma_N \equiv 2\sum_{l\epsilon N} \hat{l}^2 A^2_{Nl} \approx \frac{1}{2}\sum_{l\epsilon N} l\big(N^2 - l^2\big)\left(\frac{\hbar}{M\omega}\right)^2$$
$$= \frac{1}{16}\big(N^4 + \mathcal{O}\big(N^3\big)\big)\left(\frac{\hbar}{M\omega}\right)^2. \tag{28}$$

The simplification implied by keeping only the leading order term in N allows us to use the average sum rule $\Sigma \equiv \Sigma_{N_p}$ for the four types of particle–hole excitations that have been defined above.

The approximate diagonalization of the Hamiltonian within the RPA method is performed by solving the equation of motion

$$\big[H, \Gamma^+_t\big] = E_t \Gamma^+_t, \tag{29}$$

where Γ^+_t is the one-phonon creation operator and E_t is the energy of the one-phonon state. The main features of the RPA dispersion relations are shown in Figs. 1 (pure harmonic oscillator case) and 4 (realistic case). These dispersion relations are distinctive of asymmetric vacuum states, as in the case of pairing vibrations in normal systems [12]. They approximately show a parabolic behavior around zero and display a half-parable shape for large absolute values of the energy. Due to the existing degeneracy in the pure harmonic oscillator case, the RPA yields only two (collective) phonons Γ^+_t, $t = \pm 1$,

$$\Gamma^+_t = \lambda_{ta'j}\gamma^+_{ta'j} - \mu_{t1j}\gamma^-_{\bar{1}1j}, \tag{30}$$

with energies E_t satisfying the dispersion relation associated with the curve represented in Fig. 1. The function

$$F(\epsilon) = \frac{3}{1-\epsilon} + \frac{1}{1+\epsilon} \tag{31}$$

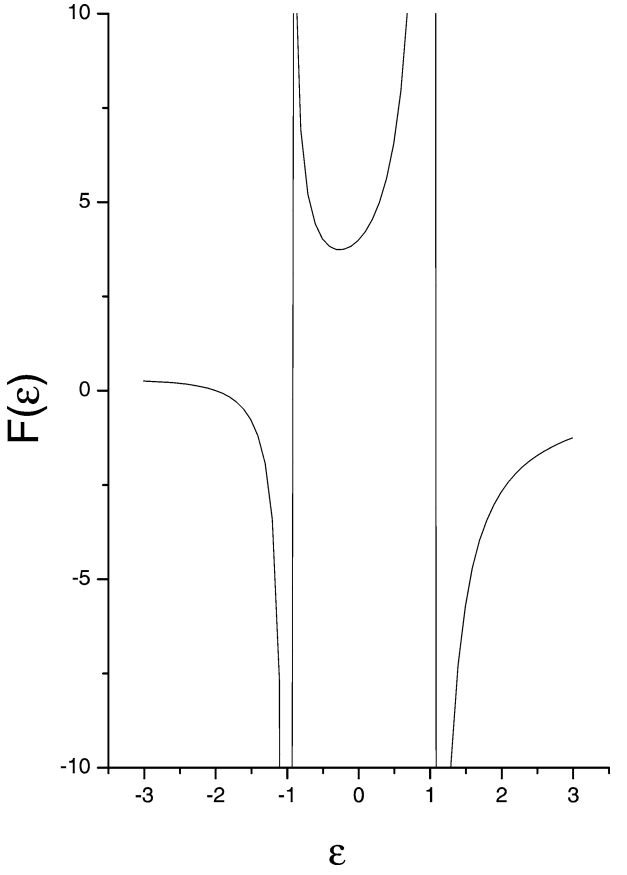

Fig. 1. The roots of the RPA dispersion relation are given by the intersection of the curve represented on the vertical axis with the horizontal line $-1/\eta$.

and the dispersion relation

$$F(\epsilon) = -\frac{1}{\eta} \tag{32}$$

are the harmonic oscillator limits of Eq. (A.12). The values of the adimensional energies $\epsilon_t \equiv E_t/2\hbar\omega$ are represented in Fig. 2 and they are given by

$$\epsilon_t = t\eta + \sqrt{\eta^2 + 4\eta + 1}, \tag{33}$$

where the adimensional parameter η is defined as $\eta \equiv \alpha\Sigma/2\hbar\omega$. The phonon amplitudes are

$$\lambda_{1a'j} = \frac{\alpha\Lambda_1}{2\hbar\omega}\hat{j}A_{a'j}/(1-\epsilon_1), \qquad \mu_{11j} = \frac{\alpha\Lambda_1}{2\hbar\omega}\hat{j}A_{pj}/(1+\epsilon_1),$$
$$\lambda_{\bar{1}1j} = \frac{\alpha\Lambda_{\bar{1}}}{2\hbar\omega}\hat{j}A_{pj}/(1-\epsilon_{\bar{1}}), \qquad \mu_{\bar{1}a'j} = \frac{\alpha\Lambda_{\bar{1}}}{2\hbar\omega}\hat{j}A_{a'j}/(1+\epsilon_{\bar{1}}), \tag{34}$$

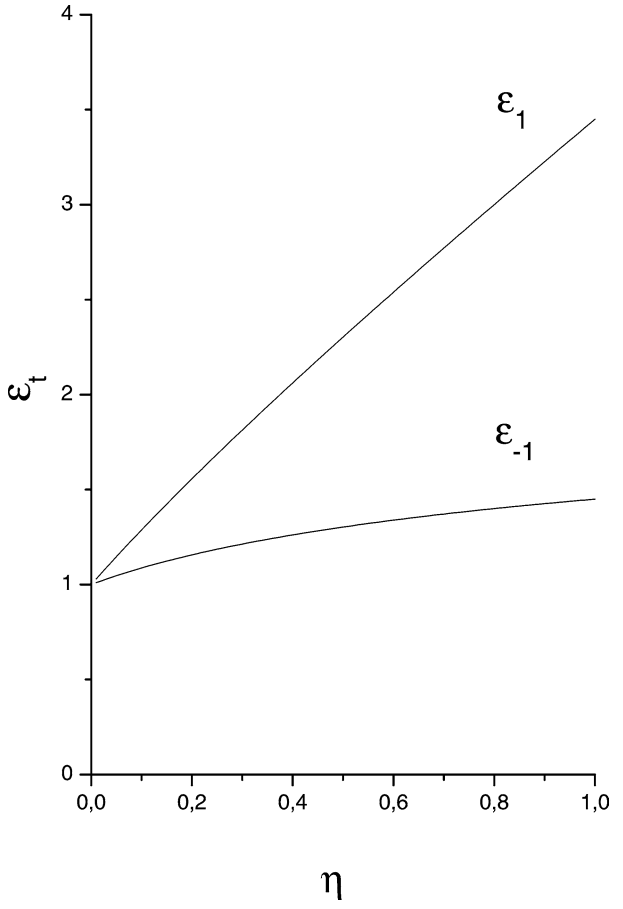

Fig. 2. Energies $\epsilon_{\pm 1}$ as a function of the parameter η.

with normalization constants

$$\Lambda_t = \sqrt{\Sigma}\sqrt{\frac{\eta + 2 + t\sqrt{\eta^2 + 4\eta + 1}}{\sqrt{\eta^2 + 4\eta + 1}}}. \tag{35}$$

We parametrize the Coulomb potential at the interior as

$$V_c(r) = \left(2.16\frac{Z}{R_0} - 0.72\frac{Z}{R_0^3}r^2\right) \text{MeV F}. \tag{36}$$

The single-particle Hamiltonian $H_{\text{sp}}^{(e)}$ includes the Coulomb contribution

$$H_{\text{sp}}^{(q)} = \left[B_N b_{Njm}^{+} b_{Njm} - \frac{0.72Z}{R_0^3} A_{Nl}\left(b_{(N+2)jm}^{+} b_{Njm} + b_{Njm}^{+} b_{(N+2)jm}\right)\right] \text{MeV F},$$

$$B_N = \frac{2.16Z}{R_0} - \frac{0.72Z}{R_0^3}\frac{\hbar}{m\omega}\left(N+\frac{3}{2}\right) \tag{37}$$

which yields the particle–hole term with isospin 1 and isospin projection 1 and the expectation value of the term with isospin 1, projection 0

$$\begin{aligned} H^{(q)}_{\mathrm{sp}11} &= \left[H^{(q)}_{\mathrm{sp}}, \tau_1\right] \to \frac{0.72Z}{R_0^3}\left(\hat{j}A_{a'l}\gamma^{+}_{1a'j} + \hat{j}A_{pj}\gamma^{-}_{\bar{1}1j}\right)\ \mathrm{MeV\,F} \\ &= \left(\frac{0.72Z}{R_0^3}\Lambda_1\Gamma^{+}_1\right)\mathrm{MeV\,F} + \cdots, \\ &= 3.12\sqrt{\frac{2+\eta+\sqrt{\eta^2+4\eta+1}}{\sqrt{\eta^2+4\eta+1}}}\Gamma^{+}_1\ \mathrm{MeV}, \\ \left\langle H^{(q)}_{\mathrm{sp}10}\right\rangle &= -\left\langle\left[H^{(q)}_{\mathrm{sp}}, \tau_1\right], \tau_{\bar{1}}\right]\right\rangle = -B_5 T = -15.93T\ \mathrm{MeV}. \end{aligned} \tag{38}$$

In the absence of $\mathbf{l}.\mathbf{s}$ and $\mathbf{l}^2$ couplings, and in the neighborhood of mass $A = 208$, shell closures take place at $Z = 70$ and $N = 112$, corresponding to an ideal $A = 182$ nucleus. In this case, $2\hbar\omega \approx 14.47$ MeV. Therefore, in the absence of the residual interaction (5) the IAS ($\omega_\xi = 15.93$ MeV) and the IMS are almost degenerate. These two states should be strongly mixed by the $H^{(q)}_{\mathrm{sp}11}$ coupling (38). Fig. 3 displays the value of the square of the admixture $|c_\xi|^2$ of the IAS in the IMS as a function of the parameter η. For values of $\eta \approx 0$, the IAS and the IMS are equally excited through a Fermi process represented by the operator $\tau_1 \to \xi^+$. However, for a more realistic IMS energy of ≈ 30 MeV, $\eta \approx 0.4$ and $|c_\xi|^2 \approx 0.1$. It means that within a pure harmonic oscillator potential, the survival of the IAS as an isolated state is preserved by the collectivity of the IMS.

5.2. Realistic single-particle basis

We start by diagonalizing a neutron and a proton Woods–Saxon potential. The parameters have been taken from Ref. [11]. The central part of the potential has the strength

$$V_0^{(p)} = -51\ \mathrm{MeV}, \qquad V_0^{(n)} = \left(-51 + 33\frac{N-Z}{A}\right)\mathrm{MeV}, \tag{39}$$

while the spin–orbit strength is

$$V_{\mathrm{so}}^{(n,p)} = -0.44V_0^{(n,p)}. \tag{40}$$

The radius R_0 and thickness a_0 are fixed at the values $1.27A^{1/3}$ F and 0.67 F, respectively. We use the Coulomb potential given in (36).

The calculations have been performed for $A = 208$. The set of 0^+ states in ^{208}Bi are described as proton (particle)–neutron (hole) excitations on the ground state of ^{208}Pb. We have included seven major harmonic oscillator shells in the calculation. A sample of single-particle energies, corresponding to the region of neutron excess, is listed in Table 1.

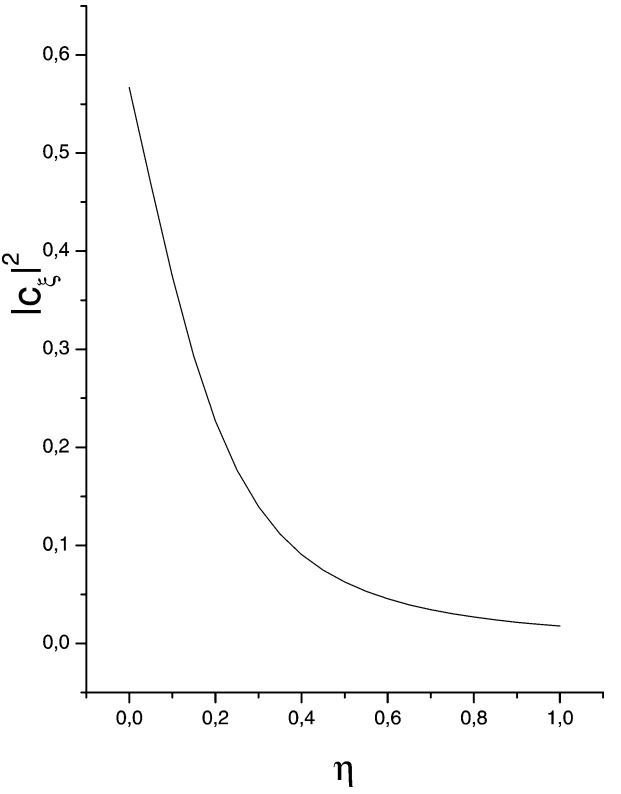

Fig. 3. Square of the amplitudes of the IAS in the IMS as a function of the parameter η.

Table 1
The eigenvalues e_{nlj} (pure Woods–Saxon potential) for neutrons, and e_{plj} (Woods–Saxon plus Coulomb potentials) for protons. The energies are in MeV. These are the states belonging to the region of neutron excess

#	lj	e_{nlj}	e_{plj}
1	$h_{9/2}$	−10.514	2.375
2	$f_{7/2}$	−9.971	3.359
3	$i_{13/2}$	−8.209	3.668
4	$f_{7/2}$	−7.794	5.693
5	$p_{3/2}$	−7.752	6.089
6	$p_{1/2}$	−6.937	6.917

The $t = 1$ ($t = -1$) particle–hole basis consists of 22 (4) states. We have obtained the value $w_\xi = 18.17$ MeV (see Eq. (19)) a value which is indeed quite comparable with the experimental value[3] $E_{\mathrm{IAS}} = 17.85$ MeV [5,13].

[3] We are given the value of the IAS energy respect to the ground state of ^{208}Pb. The experimental value $E_{\mathrm{IAS}} = 15.17$ MeV, which is the energy measured from the ground state of ^{208}Bi, is obtained after subtraction

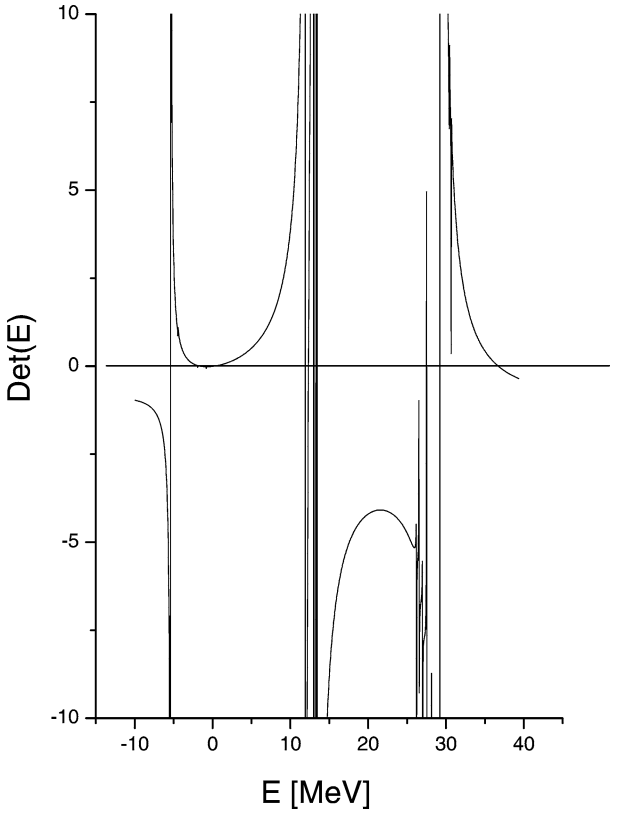

Fig. 4. RPA dispersion relation for the realistic case.

As said in the previous section, the RPA spectrum contains negative energy eigenvalues, a zero energy root and the positive energy eigenvalues, which include the $\Delta N = 0$ excitations between the single-particle states of Table 1, as well as those involving $\Delta N = 2$ transitions.

The explicit form of the RPA determinant is obtained as a straightforward generalization of Eq. (57) in I (see Appendix A). Fig. 4 shows the dispersion relation corresponding to the realistic single-particle basis. The lack of degeneracy between the particle–hole excitations manifests itself through the structure of states appearing in the region of 10–15 MeV and 26–30 MeV, as well as for negative energies. The RPA eigenvalues shown in Fig. 4 are the zeros of the determinant (A.8), calculated with $\alpha = 0.007$ MeV F^{-4}, which is equivalent to the value $\eta = \alpha\Sigma/4\hbar\omega \approx 0.4$ (see below Eq. (33)). The energy of the IMS state is given by the intersection at the far-end at about 36 MeV, which is supposed to be a realistic estimate [14]. The energy of the IMS is given in Fig. 5 for different values of the

of the neutron–proton mass difference (1.29 MeV) and the difference in the energies of the ground state of ^{208}Bi and ^{208}Pb (1.39 MeV).

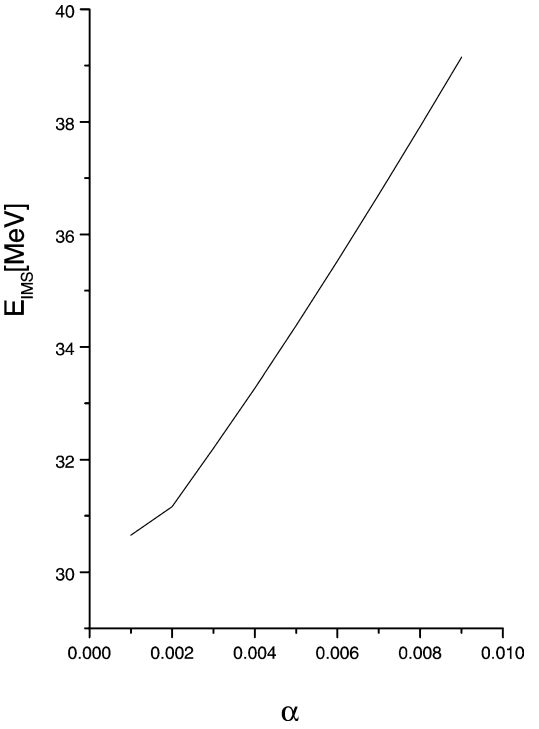

Fig. 5. Energy of the IMS as a function of the coupling constant α.

parameter α. The dependence of E_{IMS} with α is linear, for $\alpha \geqslant 0.002$ MeV F^{-4} as it was the dependence of ϵ_1 with η in the case of the pure harmonic oscillator (see Fig. 2).

5.2.1. The spreading width of the IAS

The isospin conserving Hamiltonian W gives rise to monopole RPA bosons carrying $\Delta T_z = \pm 1$. For each of these cases, there is a single giant resonance, the IMS, plus many particle–hole phonons. The Fermi population of the states with $\Delta T_z = 1$ (for instance, by means of (^{3}He, t) reactions) takes place through the admixture of each phonon with the IAS. This admixture is of the order of per tenths in the case of the IMS and of the order of per cents for the other modes.

Following the method of I, one can calculate the centroid, E_m, and the root mean square deviation, σ, associated with the population of these states

$$E_m = \frac{\sum_k E_k c_\xi^2(k)}{\sum_k c_\xi^2(k)},$$
$$\sigma = \left(\frac{\sum_k (E_k - E_m)^2 c_\xi^2(k)}{\sum_k c_\xi^2(k)} \right)^{1/2}. \tag{41}$$

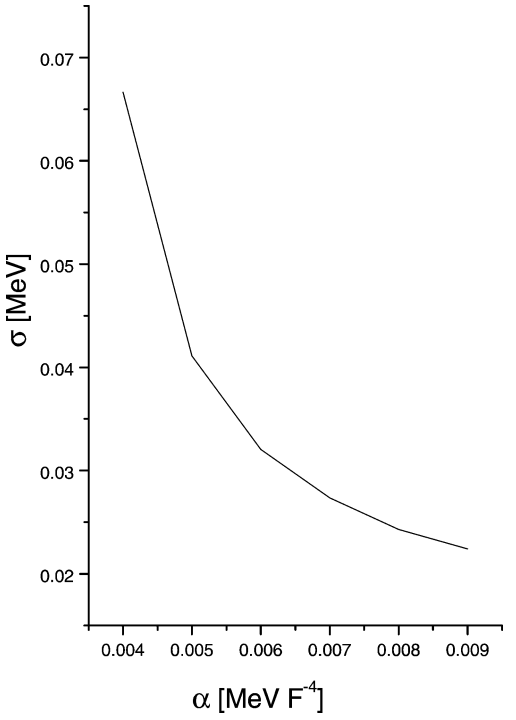

Fig. 6. Mean square deviation (σ) of the IAS due to the coupling with the $T-1$ particle–hole states as a function of the coupling constant α. The curve shows the results obtained by diagonalizing the coupling Hamiltonian of Eq. (22), excluding the IMS from the set of $T-1$ states.

The relationship between σ and the spreading width $\Gamma^{\downarrow}$ is [11,15]

$$\sigma = \frac{\Gamma^{\downarrow}\lambda}{2E_m}, \quad \lambda = \frac{Nd}{\pi}. \tag{42}$$

The quantities d and N are the mean energy spacing and the number of states, respectively.

The average excitation energy, determined from the eigenvalues and matrix elements for transitions between the perturbed states and the ground state, is almost independent of α and its value is equal to ≈ 18.31 MeV.

For $\Delta T_z = 1$ excitations, the two main peaks (IAS and IMS) are well separated. Therefore, the fragmentation of the IAS resonance over RPA configurations should be associated with the quantity σ represented in Fig. 6. Since the use of the definitions (41) is valid only for a single-mode (e.g., Gaussian-like distributions of the intensity), we have excluded the contribution of the IMS to both quantities, E_m and σ. The actual value of σ is effectively reduced by the mere existence of the IMS, since most of the strength of $T-1$ excitations around the IAS is shifted upwards due to the collective nature of the IMS. This decrease may be understood on the same basis as the change of the effective charge in E1 and E2 low-energy transitions due to the mixing between configuration particle–hole states and giant resonances: the smallness of this admixture is compensated by the large size of

the matrix element exciting the resonance. Quite systematically, this effect acts coherently for attractive forces and destructively for repulsive ones such as (5).

Due to the existence of the IMS, and in the context of the present framework, the value of σ decreases from the value ≈ 86 keV obtained in I with $\alpha = 0$, to the value $\sigma \approx 25$ keV, for $\alpha = 0.007$ MeV F^{-4}.

The strong suppression found in the present calculations suggests that higher order corrections may yield contributions of similar size, for instance those associated with transitions to two-particle–two-hole states.

The use of the relation (42), for heavy-mass nuclei, leads to the estimate $\Gamma^{\downarrow} \approx (6\text{–}12)\sigma$, i.e., a value of the order of 150–300 keV for $N = 10^6$, $d = (10\text{–}20)$ eV, $E_m = 18.31$ MeV, and $\sigma \approx 25$ keV. Although these values are about 2–3 times larger than the experimental value of the spreading width (79 ± 4 keV) [16], they are 3–4 times smaller than the value obtained with $\alpha = 0$. Further reductions could be obtained (see Fig. 6) by increasing the value of α, upon which there is no certainty. The present estimate is based on the conservative assumption that the energy of the IMS should be larger than 35 MeV. A giant resonance may also decay by particle-emission. This emission is associated with the portion of the giant resonance having the particle in the continuum [17]. Since we have not included particle states in the continuum we cannot estimate that contribution to the width.

We would like now to comment on previous attempts to explain the spreading width of the IAS in terms of the coupling to the IMS [3,4]. In these works both the energy of the IMS, $E_{\rm IMS}$ and the spreading width of the IMS at the IAS energy, $\Gamma^{\downarrow}_{\rm IMS}$, are taken as free parameters. Following [3,4] the width of the IAS is written

$$\Gamma^{\downarrow}_{\rm IAS} = \frac{1}{2T}\frac{|\langle {\rm IAS}|V_C|E_{\rm IMS}\rangle|^2}{(E_{\rm IMS} - E_{\rm IAS})^2 + (\Gamma^{\downarrow}_{\rm IMS}/2)^2}\Gamma^{\downarrow}_{\rm IMS}. \tag{43}$$

While the value of the energy of the IMS can be approximated within an interval, for instance by using the estimate discussed in [4], and the matrix element of the Coulomb interaction can be reasonably calculated, practically nothing is know about the value of the width of the IMS state at the energy of the IAS, which in the estimate of [4] is taken as $\Gamma^{\downarrow}_{\rm IMS} \approx 2\text{–}3$ MeV. In the present formalism, the only uncertainty is represented by the value of α, a value which eventually may be more accurately fixed by the experiments, while the mechanism leading to the reduction of the width of the IAS is well established and it does not require the use of additional parameters.

6. Conclusions

In this work we have extended the formalism presented in I, in order to account for the effects of the coupling between the Isobaric Analogue State and the Isovector Monopole State upon the width of the IAS. To fulfill this goal we have added, to the previously considered Hamiltonian, an interaction which induces the correlations which are specific of the IMS. The calculations have been performed in the framework of the collective treatment of the isospin degree of freedom, both for a pure harmonic oscillator and for a realistic

single particle basis. From the correspondence drawn between these set of results, we may conclude about the predominance of shell closure effects upon the structure of the IAS and of the IMS and upon the coupling between them. The coupling constant of the residual two-body interaction responsible for the appearance of the IMS was fixed by fitting the energy shift between the IMS and the IAS. To the extent that this energy shift is known, the calculations may be considered to be free of un-desired parametrizations.

It is found that, from the interplay between the strong coupling induced by the Coulomb interaction and the relatively large energy shift between the IAS and the IMS, the influence of the IMS is decisive to isolate the IAS from the background of $T-1$ particle–hole excitations. As shown by the result of our calculations the coupling between the IAS and the IMS reduces the width of the IAS by a factor four, compared to the value obtained when the coupling is ignored.

Acknowledgements

This work was supported in part by the CONICET through the Carrera del Investigador Científico; by the Fundacion Antorchas and by the University Favaloro (proyecto 010/99). We thank Prof. Juha Äystö, from ISOLDE and the University of Jyväskylä, Finland, for his interest concerning future experimental studies related to the material discussed in the present work.

Appendix A. The dispersion relation for realistic cases

The isospin conserving Hamiltonian W (20) may be written as

$$W = H^{(e)}_{\rm sp} + \frac{1}{T}\left(H^{(e)}_{\rm sp11}\tau_{\bar{1}} + H^{(e)}_{\rm sp1\bar{1}}\tau_1\right) + \frac{1}{2T^2}\langle H^{(e)}_{\rm sp10}\rangle[\tau_1,\tau_{\bar{1}}]_+ - \frac{\alpha}{2}[S_1,S_{\bar{1}}]_+ - \frac{\alpha\langle S_0\rangle}{T}(S_1\tau_{\bar{1}} + S_{\bar{1}}\tau_1) - \frac{\alpha}{2T^2}\langle S_0\rangle^2[\tau_1,\tau_{\bar{1}}]_+. \tag{A.1}$$

It is easy to verify the fact the invariance of W against isospin rotations ($[W,\tau_{\pm 1}]=0$). Within the RPA, the components of the single-particle terms are given by

$$\begin{aligned}
\tau_1 &= -\hat{j}\eta_{1aj}\gamma^+_{1aj} - \hat{j}\eta_{\bar{1}1j}\gamma_{\bar{1}1j},\\
H^{(e)}_{\rm sp} &= \Delta_{1aj}\gamma^+_{1aj}\gamma_{1aj} + \Delta_{\bar{1}1j}\gamma^+_{\bar{1}1j}\gamma_{\bar{1}1j},\\
H^{(e)}_{\rm sp11} &= -\hat{j}\Delta_{1aj}\eta_{1aj}\gamma^+_{1aj} + \hat{j}\Delta_{\bar{1}1j}\eta_{\bar{1}1j}\gamma_{\bar{1}1j},\\
\langle H^{(e)}_{\rm sp10}\rangle &= -\hat{j}^2\Delta_{1aj}\eta^2_{1aj} - \hat{j}^2\Delta_{\bar{1}1j}\eta^2_{\bar{1}1j},
\end{aligned} \tag{A.2}$$

where $a=1,2,3,4$, since we have also included the $\Delta N=0$ boson creation (and annihilation) operator

$$\gamma^+_{11j} = \frac{1}{\sqrt{2}\hat{j}}b^+_{N_njm}c_{N_njm}, \tag{A.3}$$

in addition to the $\gamma^+_{1a'j}$ phonons defined in (25), and

$$S_1 = -A_{a'j}\hat{j}\gamma^+_{1a'j} - A_{pj}\hat{j}\gamma_{\bar{1}1j},$$
$$\langle S_0\rangle = -A_{a'j}\eta_{1a'l}\hat{j}^2 + A_{pj}\eta_{\bar{1}1j}\hat{j}^2. \tag{A.4}$$

We introduce now the independent phonons

$$\Gamma^+_q = \lambda_{qaj}\gamma^+_{1aj} - \mu_{q1j}\gamma_{\bar{1}1j}. \tag{A.5}$$

The relation $[W, \Gamma^+_q] - \omega_q\Gamma^+_q$ yields the amplitudes

$$\lambda_{qaj} = \frac{\hat{j}}{\Delta_{1aj}-\omega_q}\left[\frac{K_q}{T}\left(\Delta_{1aj}\eta_{1aj} - \alpha\langle S_0\rangle A_{a'j} + \frac{\langle H^{(e)}_{\rm sp10}\rangle}{T}\eta_{1aj} - \frac{\alpha\langle S_0\rangle^2}{T}\eta_{1aj}\right)\right.$$
$$\left. + \frac{L_q}{T}\eta_{1aj} - \alpha M_q\left(A_{a'j} + \frac{\langle S_0\rangle}{T}\eta_{1aj}\right)\right],$$
$$\mu_{q1j} = \frac{\hat{j}}{\Delta_{\bar{1}1j}+\omega_q}\left[\frac{K_q}{T}\left(-\Delta_{\bar{1}1j}\eta_{\bar{1}1j} - \alpha\langle S_0\rangle A_{pj} + \frac{\langle H^{(e)}_{\rm sp10}\rangle}{T}\eta_{\bar{1}1j} - \frac{\alpha\langle S_0\rangle^2}{T}\eta_{\bar{1}1j}\right)\right.$$
$$\left. + \frac{L_q}{T}\eta_{\bar{1}1j} - \alpha M_q\left(A_{pj} + \frac{\langle S_0\rangle}{T}\eta_{\bar{1}1j}\right)\right], \tag{A.6}$$

in terms of the sums

$$K_q \equiv \hat{j}(\eta_{1aj}\lambda_{1aj} + \eta_{\bar{1}1j}\mu_{q1j}),$$
$$L_q \equiv \hat{j}(\Delta_{1aj}\eta_{1aj}\lambda_{1aj} - \Delta_{\bar{1}1j}\eta_{\bar{1}1j}\mu_{q1j}),$$
$$M_q \equiv \hat{j}(A_{a'j}\lambda_{qa'j} + A_{pj}\mu_{q1j}). \tag{A.7}$$

The RPA energies ω_{tq} are given by the roots of the determinant obtained by replacing (A.6) in (A.7), namely

$$\begin{vmatrix} \left(d_{11} - \frac{\alpha\langle S_0\rangle}{T}f\right) & d_{12} & -\alpha f \\ \left(d_{21} - \frac{\alpha\langle S_0\rangle}{T}g\right) & d_{22} & -\alpha g \\ \left(d_{31} - \frac{\alpha\langle S_0\rangle}{T}h\right) & d_{32} & (-1-\alpha h) \end{vmatrix} = 0, \tag{A.8}$$

where

$$f = X_3 + \frac{\langle S_0\rangle X_0}{T}, \qquad g = X_4 + \frac{\langle S_0\rangle X_1}{T}, \qquad h = X_5 + \frac{\langle S_0\rangle X_3}{T} \tag{A.9}$$

and

$$d_{11} = -1 + \frac{1}{T}\left(X_1 + \frac{\langle H^{(e)}_{\rm sp10}\rangle}{T}X_0\right), \qquad d_{12} = \frac{1}{T}X_0,$$
$$d_{21} = \frac{1}{T}\left(X_2 + \frac{\langle H^{(e)}_{\rm sp10}\rangle}{T}X_1\right), \qquad d_{22} = -1 + \frac{1}{T}X_1,$$
$$d_{31} = \frac{1}{T}\left(X_4 + \frac{\langle H^{(e)}_{\rm sp10}\rangle}{T}X_3\right), \qquad d_{32} = \frac{1}{T}X_3. \tag{A.10}$$

The quantities X_n are defined as in I, with modifications due to the inclusion of the IMS interaction,

$$X_0 = \hat{j}^2\left(\frac{\eta_{1aj}^2}{\Delta_{1aj}-\omega_q}+\frac{\eta_{\bar{1}1j}^2}{\Delta_{\bar{1}1j}+\omega_q}\right), \qquad X_1 = \hat{j}^2\left(\frac{\Delta_{1aj}\eta_{1aj}^2}{\Delta_{1aj}-\omega_q}-\frac{\Delta_{\bar{1}1j}\eta_{\bar{1}1j}^2}{\Delta_{\bar{1}1j}+\omega_q}\right),$$

$$X_2 = \hat{j}^2\left(\frac{\Delta_{1aj}^2\eta_{1aj}^2}{\Delta_{1aj}-\omega_q}+\frac{\Delta_{\bar{1}1j^2}\eta_{\bar{1}1j}^2}{\Delta_{\bar{1}1j}+\omega_q}\right), \qquad X_3 = \hat{j}^2\left(\frac{A_{a'j}\eta_{1a'j}}{\Delta_{1a'j}-\omega_q}+\frac{A_{pj}\eta_{\bar{1}1j}}{\Delta_{\bar{1}1j}+\omega_q}\right),$$

$$X_4 = \hat{j}^2\left(\frac{A_{a'j}\Delta_{1a'j}\eta_{1a'j}}{\Delta_{1a'j}-\omega_q}-\frac{A_{pj}\Delta_{\bar{1}1j}\eta_{\bar{1}1j}}{\Delta_{\bar{1}1j}+\omega_q}\right),$$

$$X_5 = \hat{j}^2\left(\frac{A_{a'j}^2}{\Delta_{1a'j}-\omega_q}+\frac{A_{pj}^2}{\Delta_{\bar{1}1j}+\omega_q}\right). \tag{A.11}$$

After some straightforward algebra, the determinant is cast in the form of the dispersion relation

$$-\frac{1}{\alpha} = \frac{Y_\omega}{Z_\omega}, \tag{A.12}$$

where

$$\begin{aligned} Y_\omega &= f(d_{21}d_{32}-d_{22}d_{31}) + g(d_{12}d_{31}-d_{11}d_{32}) \\ &\quad + h(d_{11}d_{22}-d_{12}d_{21}) + \frac{\langle S_0\rangle}{T}(gd_{12}-fd_{22}), \\ Z_\omega &= d_{11}d_{22}-d_{12}d_{21}. \end{aligned} \tag{A.13}$$

References

[1] D.R. Bes, O. Civitarese, Nucl. Phys. A 732 (2004) 49.
[2] N. Auerbach, J. Hüfner, A.K. Kerman, C.M. Shakin, Rev. Mod. Phys. 44 (1972) 48; A.Z. Mekjian, Phys. Rev. Lett. 25 (1970) 888.
[3] N. Auerbach, Phys. Lett. B 44 (1973) 241.
[4] N. Auerbach, Phys. Rep. 98 (1983) 274.
[5] J. Jänecke, M.N. Harakeh, S.Y. Van der Werf, Nucl. Phys. A 463 (1987) 571.
[6] N. Auerbach, A. Klein, Nucl. Phys. A 395 (1983) 77.
[7] D.R. Bes, J. Kurchan, The Treatment of Collective Coordinates in Many-Body Systems, World Scientific, Singapore, 1990.
[8] D.R. Bes, O. Civitarese, Phys. Rev. C 63 (2001) 044323.
[9] E.R. Marshalek, Phys. Rev. C 11 (1975) 1426.
[10] D.R. Bes, O. Civitarese, Nucl. Phys. A 705 (2002) 297.
[11] Aa. Bohr, B. Mottelson, Nuclear Structure, vol. I, Benjamin, New York, 1969.
[12] D.R. Bes, R.A. Broglia, Nucl. Phys. 80 (1966) 289.
[13] M.S. Antony, J. Britz, A. Pape, At. Data Nucl. Data Tables 40 (1988) 9; L. Britz, A. Pape, M.S. Antony, At. Data Nucl. Data Tables 68 (1) (1998) 126.
[14] Aa. Bohr, J. Damgaard, B.R. Mottelson, in: A. Jossain, et al. (Eds.), Nuclear Structure, North-Holland, Amsterdam, 1967, p. 1.
[15] A. Molinari, H. Weidenmüller, nucl-th/0403038.
[16] H. Akimune, et al., Nucl. Phys. A 569 (1994) 255c.
[17] J. Blomqvist, et al., Phys. Rev. C 53 (1996) 2001.